aerospace

MDPI

Article

Design of Orbit Controls for a Multiple CubeSat Mission Using Drift Rate Modulation

Youngbum Song, Sang-Young Park *, Geuk-Nam Kim and Dong-Gu Kim

Astrodynamics and Control Laboratory, Department of Astronomy, Yonsei University, Seoul 03722, Korea; song0bum@yonsei.ac.kr (Y.S.); south920528@gmail.com (G.-N.K.); donggu87@gmail.com (D.-G.K.)
* Correspondence: spark624@yonsei.ac.kr

Abstract: For the low-cost improvement of laser communication, which is critical for various applications such as surveillance systems, a study was conducted on relative distance control based on orbital drift rate modulations for multiple CubeSats during formation flying. The VISION mission covered in this paper comprises two CubeSats to demonstrate laser communication technology in space. During the mission, the deputy CubeSat changes the relative distance to execute mission objectives within various scenarios. Impulsive controls decrease, maintain, and increase the relative distance between the CubeSats by changing the orbital drift rates. The simulation results indicated that the desired orbital operation can be conducted within a given ΔV budget. In addition, the errors in the orbit determination, thrust maneuvers, and time synchronization were analyzed to satisfy the mission requirements. The mass-to-area ratio should be matched to adjust the relative distance between satellites with different properties by drift rate modulation. The proposed orbit control method appropriately operated the VISION mission by adjusting the drift rate modulation. The results of this study serve as a basis for the development of complex orbit control simulations and detailed designs that reflect the characteristics of the thrust module and operational aspects.

Keywords: CubeSat; orbital drift rate; formation flying; orbit control

Citation: Song, Y.; Park, S.-Y.; Kim, G.-N.; Kim, D.-G. Design of Orbit Controls for a Multiple CubeSat Mission Using Drift Rate Modulation. *Aerospace* **2021**, *8*, 323. https://doi.org/10.3390/aerospace8110323

Academic Editor: Fu-yuen Hsiao

Received: 15 September 2021
Accepted: 27 October 2021
Published: 29 October 2021

1. Introduction

Laser communication systems enhance the size, weight, and power efficiency compared to traditional radiofrequency RF systems at a low cost [1]. In addition, there are no regulatory constraints on the licensing of frequency bands, which is helpful for establishing low earth orbit mega constellations [2]. The advantages of laser communication include commercial and defense applications and high-speed data relay in remote sensing or surveillance systems [3]. By utilizing CubeSat platforms, key technologies for space-to-space laser communication can be realized on-orbit at a low development cost. The CubeSat Laser Infrared CrosslinK (CLICK-B/C) denotes a technology demonstration mission using two CubeSats for the laser crosslink within a range of 25–500 km. In this mission, the data communication speed using laser communication was 50 Mbps. Given that there was no thruster for the mission, a differential air drag control was used to roughly adjust the relative distance [4]. As a National Aeronautics and Space Administration (NASA) program, AeroCube-7B/C demonstrated a precise pointing system with miniaturized actuators and sensors for the laser crosslink. Given that the thruster mounted on this mission was additionally for technical verification, the relative distance for laser communication was controlled using differential air drag control [5]. Moreover, LINCS-A and LINCS-B aim to realize laser communication at a data transfer rate of 5 Gbps and relative distance of up to 2000 km. This mission was not equipped with a thruster; thus, the relative distance was adjusted using differential air drag control [6].

To implement laser communication and demonstrate several space technologies, this paper proposes a high-speed inter-satellite communication system using an infrared optical terminal and nanosatellite mission. The objective of the mission was to establish and

validate a high-speed laser crosslink system using the formation flying of two 6U CubeSats. The final objective was to achieve a data transfer rate of 1 Gbps with a coded bit error rate (BER) of less than 10^{-9} at an inter-satellite distance of up to 1000 km. Figure 1 presents a conceptual illustration of the VISION mission. The laser communication system between the two CubeSats of the mission was half the mass and size of the LINCS system, which demonstrated the same inter-satellite link performance. To reduce the geometric loss by increasing the diameter of the laser communication receiver, a deployable optical system was introduced. Research on space-deployable optical systems has been carried out for the miniaturization and weight reduction of high-resolution earth observation payloads [7]. Precise and rapid orbital adjustment is required for the operation of optical communication-based satellite constellations. Therefore, the positions of the CubeSats in the VISION mission should be relocated, and the relative distance between the satellites should be adjusted by thrusters mounted on the satellites.

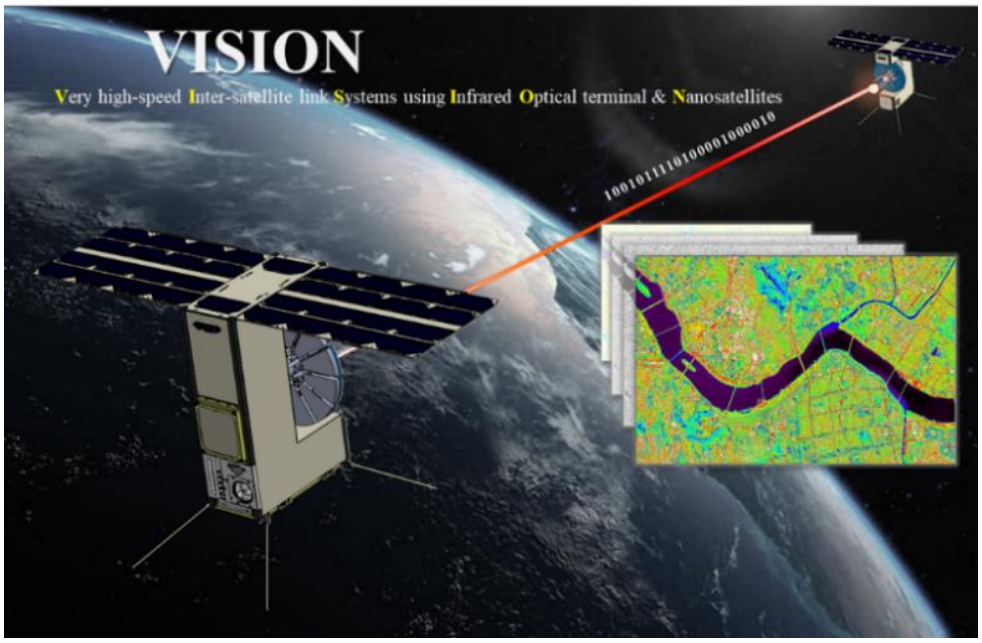

Figure 1. Conceptual illustration of VISION mission. The mission demonstrates laser communication between CubeSats at various relative distances.

To verify laser communication, the CubeSats of the VISION mission should be located within a specific orbit. When sunlight is directly incident on the optical system for laser communication, noise increases in the communication; thus, CubeSats should be located in the orbit wherein the minimum sunlight is incident on the optical system during the laser communication. As the link budget decreases due to a decrease in the laser intensity with an increase in distance, the increase in the relative distance between the CubeSats can be analyzed to determine the influence of laser communication on the relative distance. As the distance between satellites increases, the free-space path loss increases. To demonstrate laser communication at various relative distances, the two CubeSats should be capable of changing their relative distance via orbit control. In the CANYVAL-X mission, two CubeSats decreased the relative distance using differential air drag control to demonstrate the vision alignment system, which is a core technology of the virtual space telescope [8]. GomX-4A and GomX-4B decreased the relative distances by changing altitude using thrust [9]. To gradually change and maintain the relative distance over several days, the VISION mission utilizes drift rate modulation. The drift rate modulation is to adjust the drift rate, which is the angular speed at which the satellite moves in the orbital plane, using orbit control. The SNIPE mission uses drift rate modulation to gradually change the relative distance between the CubeSats. In this mission, the difference in the J_2

perturbations between the CubeSats was used to decrease the relative distance on a similar orbital plane [10]. Different from the SNIPE mission, the VISION mission requires precise relative distance maintenance. In the VISION mission, the drift rate modulation using the J_2 perturbations can change the relative distance over long periods of time using less fuel. In addition, this method can maintain the relative distance within a few kilometers without determining the relative orbit. Through drift rate modulation, the requirements for repeatedly decreasing and increasing relative distance and precise relative distance maintenance were analyzed for the VISION mission.

This paper presents orbit control scenarios for the VISION mission and an orbit control method for orbital operation. This paper assumes $\boldsymbol{\Delta V}$ as impulsive burn to check whether orbit operation is possible within $\boldsymbol{\Delta V}$ budget before selecting a thrust module. In addition, we present the allowable error range of thrust module and the error range of orbit information for the mission. Orbital controls perform the mission by adjusting the CubeSat orbital drift rate, which is influenced by orbital perturbations. The orbital drift rate refers to the angular speed at which a satellite moves in an orbital plane. Thus, the drift rate modulation changes the relative speed of one CubeSat with respect to the other CubeSat by adjusting the angular speed. By comparing the zonal harmonics' terms that influence the drift rate of the CubeSats, the influences of the terms on the mission were analyzed. Based on numerical simulations results, the orbital operation can realize the objectives of the VISION mission using the proposed orbit control method. The numerical simulations verified that the orbital operation can be established within a limited $\boldsymbol{\Delta V}$ budget. In addition, the influences of the mission by the orbit determination error, magnitude and direction error of thrust, and time synchronization error were analyzed. It was found that even if the masses and areas of the satellites are different, the relative distance can be adjusted by applying drift rate modulation by matching a specific mass-to-area ratio between two satellites.

Section 2 presents the requirements for orbit control and the proposed orbit control method for the modulation of the relative distance. Section 3 proposes orbit control scenarios to demonstrate the laser communication and $\boldsymbol{\Delta V}$ calculation method according to the orbit control types. The numerical simulation and error analysis results for the orbit control are presented in Section 4. In addition, Section 4 presents the simulation results of the relative distance controls when the physical properties of the satellites were different. Section 5 presents the conclusions and applications of this study.

2. Problem Statements for VISION Mission

2.1. Coordinate System

An inertial coordinate system is used to express the state vectors of the two CubeSats, namely, $[\mathbf{I}, \mathbf{J}, \mathbf{K}]$, as shown in Figure 2. The origin of the coordinate system is the center of the Earth, and the fundamental plane is the equatorial plane. The **I** axis is parallel to the vernal equinox direction, and the **K** axis is directed toward the North pole. In addition, the local vertical and local horizontal (LVLH) coordinate system and relative coordinate system are used to express $\boldsymbol{\Delta V}$ for orbit control. Moreover, $[\mathbf{R}, \mathbf{S}, \mathbf{W}]$ in Figure 2 represents the LVLH coordinate system. The origin of the coordinate system is the center of the satellite, and the fundamental plane is the same as that of the orbital plane. The **R** axis is parallel to the radial vector, which is from the origin of the Earth to the center of the satellite. The **S** axis is perpendicular to the radial vector, and points along the direction of the satellite velocity in the case of circular orbit, and the **W** axis is parallel to the angular momentum vector of the orbit [11].

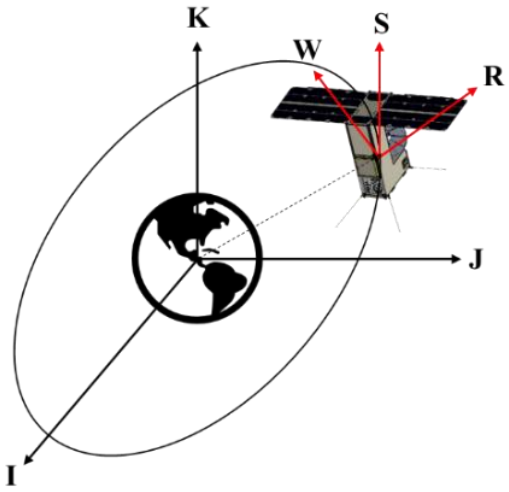

Figure 2. Definition of the coordinate systems. The inertial coordinate system ([**I,J,K**] in the figure) is used to express the state vectors of two CubeSats, and the relative coordinate system [**R,S,W**] is used to derive $\mathbf{\Delta}\boldsymbol{V}$ for orbit control.

2.2. Requirements in Orbit Controls

The VISION mission verifies optical communication technologies between two CubeSats in space using lasers. When sunlight is incident on the optical system of the laser communication scheme, noise is generated in the inter-satellite link. To minimize the noise caused by sunlight, the orbit of the CubeSats should be perpendicular to the sun vector, as shown in Figure 3. In particular, the relative position vector of the two CubeSats is perpendicular to the sun vector. Therefore, the local time of the ascending node (LTAN) of the orbit is either 90° or 270°. In addition, the orbit is required to be a sun-synchronous orbit, to ensure that the noise due to the sun is approximately constant while demonstrating the laser communication by maintaining the incident angle of the sunlight on the orbital surface. Given that the laser intensity is inversely proportional to the square of the distance, the intensity of the laser that reaches the receiving CubeSat decreases as the distance increases. Given that the laser intensity influences the link budget, a decrease in the received laser intensity indicates a loss of communication. With a decrease in the distance, the signal increases; thus, the laser communication was tested by increasing the relative distance, as shown in Figure 4. In addition, the demonstration was performed while maintaining various relative distances for 10 days at each desired relative distance. A duration of 10 days is required to correct the attitudes of the CubeSats, which have a significant influence on the laser communication, and to demonstrate five cycles of laser communication. We intended to calibrate the beam-directing system and the threshold for laser detection by the detector according to the SNR requirement based on the results of laser communication operation repeatedly performed at the same distance. It was decided in five cycles, considering the limited system size, operating life, and thrust. The performance of the laser communication system can be precisely verified when the loss due to the distance is equal. Based on the optical link budget design, the signal loss due to distance error was limited to 3 dB. In the case of 50 km, the distance error of $\pm$8.5 km yielded 3-dB signal loss, but for the convenience of defining requirements in the conceptual design stage, it was unified to $\pm$10 km. Therefore, the relative distance was maintained within $\pm$10 km to equalize the loss by distance. Therefore, the laser communication system should be verified while maintaining the desired relative distances within $\pm$10 km for 10 days.

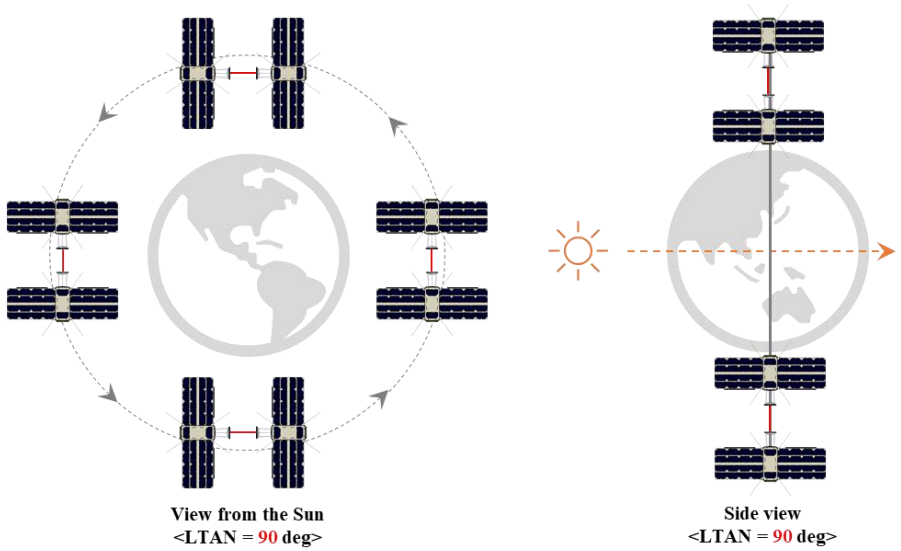

Figure 3. Requirement in local time of ascending node. To minimize the noise in the laser communication by sunlight, the orbital plane should be perpendicular to the sun vector.

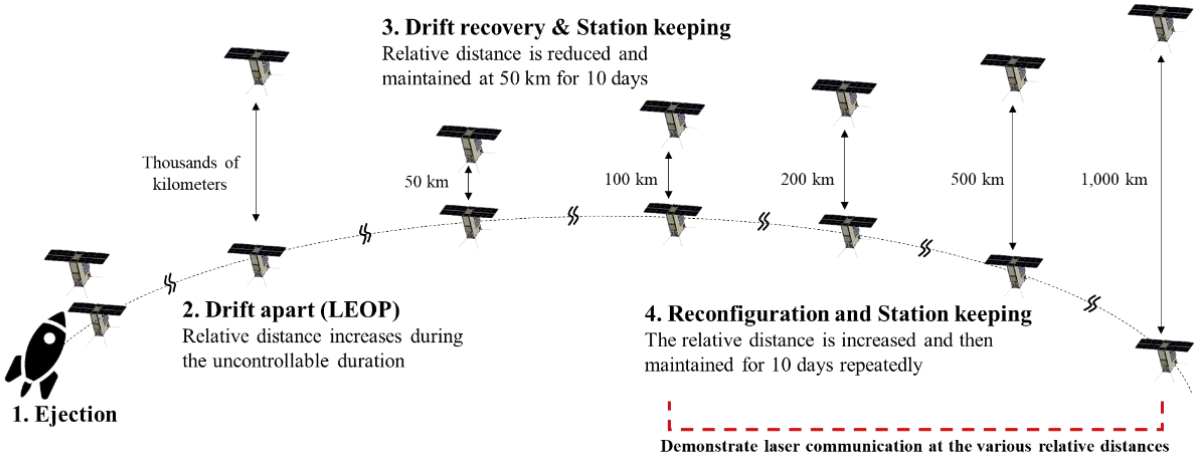

Figure 4. Orbital operation for VISION mission. The two CubeSats maintained various relative distances and demonstrate laser communication for 10 days at each distance.

To demonstrate laser communication in orbit, in the mission, two 6U CubeSats changed their relative distance according to the operation, which was divided into three phases, as shown in Figure 4. Two CubeSats were inserted into orbit by a launch vehicle, and performed initialization, stabilization, and commissioning in the launch and early orbit phase (LEOP). Orbit control was unavailable until a month after the commissioning of the sensors and actuators. After preparing the orbit control, the two CubeSats entered the drift recovery phase, thus reducing their relative distance. Subsequently, in the mission phase, the relative distance was repeatedly changed and maintained to demonstrate the laser communication at various relative distances.

The relative distance between the two CubeSats varied during the lifetime of the VISION mission. Figure 5 presents the desired changes in relative distance over time by orbit control. Three types of orbit controls, namely, drift recovery, station keeping, and reconfiguration, were utilized to operate the orbits. In the drift recovery phase, the relative distance was reduced to 50 km, which was the first set point in 30 days, and then maintained for 10 days by impulsive control. The set points were sequentially increased to 100 km, 200 km, 500 km, and 1000 km to demonstrate the laser communication at various relative distances in the mission phase. In addition, the distances should be

maintained within ±10 km for each demonstration duration, as indicated by the gray area in Figure 5. This is to evaluate the laser communication performance by fixing the distance, which influences the communication strength. The demonstration and reconfiguration duration should be repeated during the mission phase to maintain and increase the relative distance, respectively.

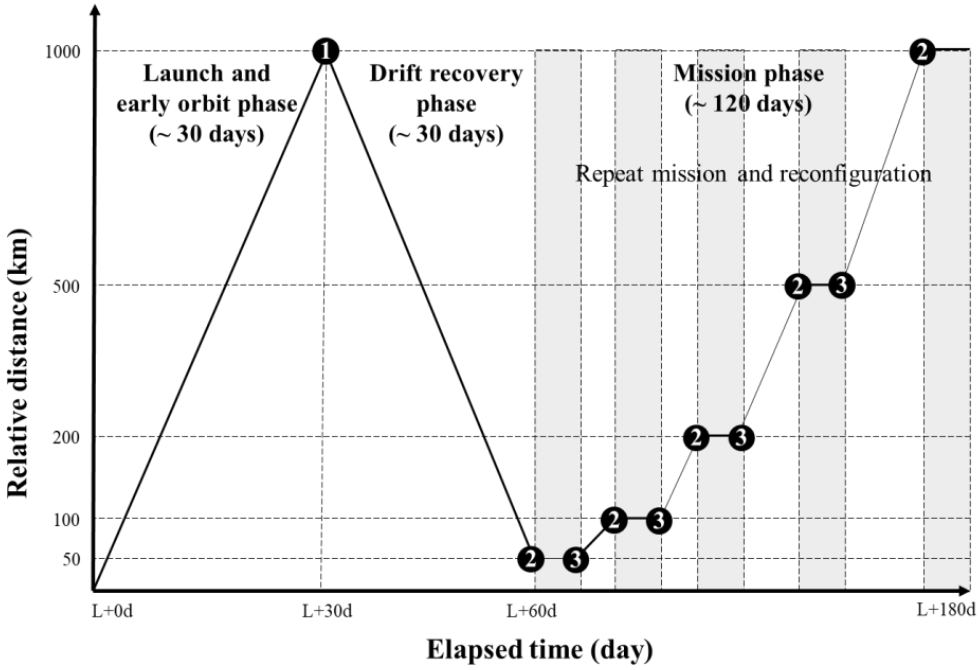

Figure 5. Conceptual illustration of desired changes in the relative distance over time between two CubeSats. The relative distance increased within the uncontrollable duration of the launch and early orbit phase. The relative distance was decreased and maintained at 50 km to demonstrate the laser communication. The distance was then increased and maintained by orbit controls. The circle markers indicate the orbit controls. The numbers 1, 2, and 3 indicate drift recovery, station keeping, and reconfiguration, respectively.

2.3. Orbit Control Scenarios

Figure 6 presents a flowchart of the numerical simulations of the orbit control scenarios for the VISION mission. Two CubeSats (a reference CubeSat and a deputy CubeSat) were separated after ejection from a single launch vehicle by the relative velocity due to the ejection. After initialization, stabilization, and commissioning, the deputy CubeSat controlled its orbit to decrease the relative distance with respect to the reference CubeSat. When the relative distance was 50 km after the drift recovery, the demonstration mission was performed while maintaining the relative distance through the orbit control for station keeping. The relative distance was maintained within 10 km for 10 days. Thereafter, orbit control for the reconfiguration was executed to increase the relative distance until the subsequent set point during the transfer time between the set points. The transfer times between the set points were set based on the mission lifetime. When the relative distance reached the subsequent set point, the orbit control for station keeping maintained the relative distance for 10 days. The reconfiguration and station keeping were repeated for the transition to the subsequent set point. The orbit controls were repeated to increase and maintain the relative distance in the order of 100 km, 200 km, 500 km, and 1000 km.

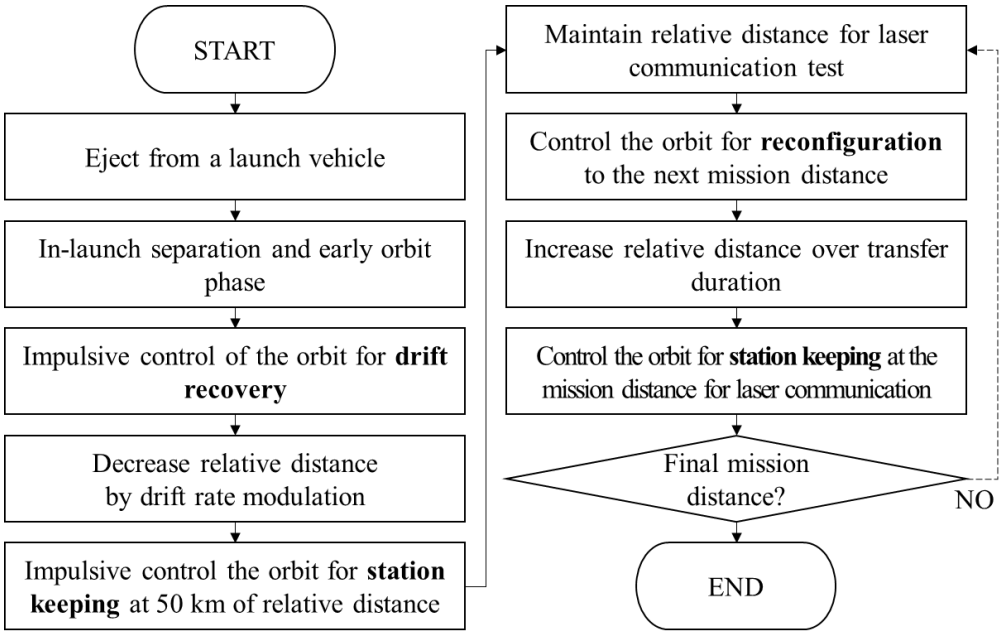

Figure 6. Flowchart for the numerical simulations of the orbit control scenarios for the VISION mission. The relative distance is modulated by three types of orbit controls: drift recovery, station keeping, and reconfiguration.

3. Materials and Methods

3.1. Drift Rate Equation

The relative distance between two CubeSats vary from thousands of kilometers over tens of days after ejection from a launch vehicle. The Cartesian elements, position, and velocity are difficult to utilize for orbit control over tens of days due to their large variations with time. Thus, we introduced Keplerian elements to derive orbit controls for their gradual changes according to the changes in the relative distance. Orbital perturbations were utilized to gradually adjust the relative distance over a long period of time. Lagrange planetary equations (LPEs) described the time derivative of the orbital elements by conservative perturbations [11]. Secular changes in orbital elements caused by J_2 perturbations can be analytically described using LPEs. The sum of secular changes caused by the J_2 perturbations of the argument of perigee (AoP) and mean anomaly (MA) is referred to as the drift rate ($\dot{\lambda}$), which is the time derivative of the argument of latitude (AoL, λ). AoL can be approximated by the sum of AoP and MA for the near-circular orbit. The AoL is the sum of AoP and mean anomaly, which indicates the angle of a satellite position from the ascending node in the orbital plane. Equation (1) is the drift rate ($\dot{\lambda}$) equation, which is a function of the semi-major axis (SMA, a), eccentricity (ECC, e), and inclination (INC, i) [10].

$$\dot{\lambda}(a,e,i) = \dot{\omega} + \dot{M}_0 + n = \frac{3n\,J_2 R_E^2}{4p^{\,2}}\left(4 - 5\sin^2 i\,\right) + \frac{3n\,J_2 R_E^2\sqrt{1-e^{\,2}}}{4p^{\,2}}\left(2 - 3\sin^2 i\,\right) + \sqrt{\frac{\mu}{a^3}} \quad (1)$$

where ω is the argument of perigee, $\dot{M}_0$ is the mean anomaly at an epoch, n is the mean motion, J_2 is the gravity coefficient of the J_2 perturbation, R_E is the mean Earth radius, $p = a(1-e^2)$ is a semi-parameter, and μ is the gravitational parameter for the Earth.

To improve the precision of the drift rate, other high-order terms of the drift rate equation can be considered. The nonlinear term for J_2 and the linear terms for J_4 and J_{26} were derived in [11]. The high-order terms are smaller than the standard deviation of the drift rate within one orbital period, as derived based on the mean orbital elements. Therefore, only the linear term for J_2 was considered to calculate the drift rate in this study.

3.2. Change in Drift Rate by Orbit Control

Gauss's variational equations (GVEs) were utilized to modulate the drift rate by changing the orbital elements by impulsive burn. Moreover, GVEs describe the time derivative of orbital elements by non-conservative perturbations. The discretized GVEs for the SMA, ECC, and INC are as follows [12]:

$$\begin{aligned} \delta a &= \tfrac{2}{n\sqrt{1-e^2}}\{e\sin\nu\boldsymbol{\Delta V_R} + (1+e\cos\nu)\boldsymbol{\Delta V_S}\} \\ \delta e &= \tfrac{\sqrt{1-e^2}}{na}\left\{\sin\nu\boldsymbol{\Delta V_R} + \left(\cos\nu + \tfrac{e+\cos\nu}{1+e\cos\nu}\right)\boldsymbol{\Delta V_S}\right\} \\ \delta i &= \tfrac{\sqrt{1-e^2}\cos\lambda}{na(1+e\cos\nu)}\boldsymbol{\Delta V_W} \end{aligned} \tag{2}$$

where ν is the true anomaly, and $\boldsymbol{\Delta V_R}$, $\boldsymbol{\Delta V_S}$, and $\boldsymbol{\Delta V_W}$ are components of $\boldsymbol{\Delta V}$ along each axis of the LVLH coordinate system. By linearizing the drift rate equation with respect to the SMA, ECC, and INC, the changes in drift rate according to changes in orbital elements can be expressed analytically, as expressed by Equation (3), which was derived in [10].

$$\partial\dot{\lambda} = \tfrac{\partial\dot{\lambda}}{\partial a}\partial a + \tfrac{\partial\dot{\lambda}}{\partial e}\partial e + \tfrac{\partial\dot{\lambda}}{\partial i}\partial i$$

with

$$\begin{aligned} \tfrac{\partial\dot{\lambda}}{\partial a} &= \tfrac{21J_2R_E^2\sqrt{\mu}}{8(1-e^2)^2a^{9/2}}\left(4-5\sin^2 i\right) + \tfrac{21J_2R_E^2\sqrt{\mu}}{8(1-e^2)^{3/2}a^{9/2}}\left(2-3\sin^2 i\right) + \tfrac{3\sqrt{\mu}}{2a^{5/2}} \\ \tfrac{\partial\dot{\lambda}}{\partial e} &= \tfrac{3J_2R_E^2e\sqrt{\mu}}{a^{7/2}(1-e^2)^3}\left(4-5\sin^2 i\right) + \tfrac{9J_2R_E^2e\sqrt{\mu}}{4a^{7/2}(1-e^2)^{5/2}}\left(2-3\sin^2 i\right) \\ \tfrac{\partial\dot{\lambda}}{\partial i} &= \tfrac{3J_2R_E^2\sqrt{\mu}}{4a^{7/2}(1-e^2)^2}\left(-5-3\sqrt{1-e^2}\right)\sin 2i \end{aligned} \tag{3}$$

By combining the discretized GVEs and linearized drift rate equation, the changes in the drift rate ($\delta\dot{\lambda}$) due to $\boldsymbol{\Delta V}$ are analytically described in Equation (4). Equation (4) was used to calculate $\boldsymbol{\Delta V}$ for the desired changes in the drift rate of the deputy CubeSat by multiplying both sides by the inverse of the coefficient matrix.

$$\delta\dot{\lambda} = \begin{bmatrix} \frac{\partial\dot{\lambda}}{\partial a} & \frac{\partial\dot{\lambda}}{\partial e} & \frac{\partial\dot{\lambda}}{\partial i} \end{bmatrix} \begin{bmatrix} \frac{2e\sin\nu}{n\sqrt{1-e^2}} & \frac{2(1+e\cos\nu)}{n\sqrt{1-e^2}} & 0 \\ \frac{\sqrt{1-e^2}\sin\nu}{na} & \frac{\sqrt{1-e^2}}{na}\left(\cos\nu + \frac{e+\cos\nu}{1+e\cos\nu}\right) & 0 \\ 0 & 0 & \frac{\sqrt{1-e^2}\cos\lambda}{na(1+e\cos\nu)} \end{bmatrix} \begin{bmatrix} \boldsymbol{\Delta V_R} \\ \boldsymbol{\Delta V_S} \\ \boldsymbol{\Delta V_W} \end{bmatrix} \tag{4}$$

3.3. Desired Change in the Drift Rate of Deputy CubeSat

The two CubeSats were identical. However, as a result of commissioning, the CubeSat with the superior thruster performance was set as a deputy CubeSat and the other was set as a reference CubeSat. The desired change in the drift rate of the deputy CubeSat was derived using three approaches. First, for the drift recovery denoted as 1 in Figure 5, the desired change in the drift rate of deputy CubeSat was derived to decrease the relative distance with respect to the reference CubeSat for a certain duration. Based on the drift rate of the reference CubeSat, the desired change in the drift rate was determined such that the drift rate of the deputy CubeSat was a value that reduced the AoL difference with respect to the reference CubeSat for the certain duration. The orbit control acted to reduce the increased relative distance during the uncontrollable duration after ejection. The desired change in the drift rate was calculated to reduce the difference in AoL between the two CubeSats for 30 days, as expressed by Equation (5).

$$\delta\dot{\lambda}_{DR} = \dot{\lambda}_{ref} - \dot{\lambda}_{dep} + \frac{\Delta\lambda}{t_{DR}}$$

with

$$\Delta\lambda = \begin{cases} -\left(2\pi + \lambda_{dep} - \lambda_{ref}\right) & , -2\pi \leq \lambda_{dep} - \lambda_{ref} < -\pi \\ -\left(\lambda_{dep} - \lambda_{ref}\right) & , -\pi \leq \lambda_{dep} - \lambda_{ref} \leq \pi \\ 2\pi + \lambda_{dep} - \lambda_{ref} & , \pi < \lambda_{dep} - \lambda_{ref} < 2\pi \end{cases} \quad (5)$$

where $\delta\dot{\lambda}_{DR}$ is the desired change in the drift rate of the deputy CubeSat for drift recovery, $\dot{\lambda}_{ref}$ and $\dot{\lambda}_{dep}$ are the drift rates of the reference and deputy CubeSats, respectively, $\Delta\lambda$ is the relative AoL that requires changing, t_{DR} is the duration of the drift recovery, and λ_{ref} and λ_{dep} are the AoL of the reference and deputy CubeSats, respectively. In addition, $\Delta\lambda$ was calculated by dividing the range to decrease the relative AoL by the orbit controls, and $\delta\dot{\lambda}_{DR}$ was calculated at the time of orbit control.

Second, for the station keeping to maintain the relative distance, which is marked as 2 in Figure 5, the drift rate of the deputy CubeSat was equal to the drift rate of the reference CubeSat. The orbit control matched the drift rates of the two CubeSats to maintain their relative distance. The desired change in the drift rate of the deputy CubeSat for the station keeping was expressed as Equation (6) and occurred to obtain the same drift rate for the two CubeSats.

$$\delta\dot{\lambda}_{SK} = \dot{\lambda}_{ref} - \dot{\lambda}_{dep} \quad (6)$$

Third, the orbit control for reconfiguration, which is marked as 3 in Figure 5 and changed the relative distance to the subsequent set point, changed the drift rate of the deputy CubeSat to increase the relative distance between the set points during the data transfer duration. The desired change in the AoL between the two CubeSats ($\delta\lambda_{trans}$) corresponding to the required change in the relative distance for the subsequent set point was calculated by approximation, as expressed by Equation (7), given that the SMA was significantly large when compared with the relative distance that requires changing.

$$\delta\lambda_{trans} \cong 2\sin^{-1}\frac{\Delta d}{2a} \quad (7)$$

where Δd is the difference between the current set point and the subsequent set point and Δd is significantly small when compared with the SMA. The geometrical description of $\delta\lambda_{trans}$ is shown in Figure 7. Therefore, the desired change in the drift rate of the deputy CubeSat for reconfiguration was calculated using Equation (8). The drift rate of the deputy CubeSat after the reconfiguration caused a difference in the AoL with respect to the reference CubeSat, which corresponded to the subsequent set point during the data transfer duration.

$$\delta\dot{\lambda}_{rec} = \dot{\lambda}_{ref} - \dot{\lambda}_{dep} + \frac{\delta\lambda_{trans}}{t_{trans}} \quad (8)$$

where t_{trans} is the transfer time between the current and the subsequent set point.

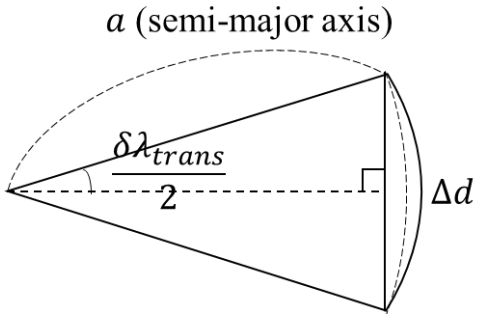

Figure 7. Geometrical description of $\delta\lambda_{trans}$ corresponding to the difference between the set point for the reconfiguration phase.

One impulsive burn caused the desired change in the drift rate for each orbit control. After calculating the desired change in the drift rate according to the objective of each orbit control based on Equations (5), (6), and (8), ΔV was calculated using the orbital elements at the instant at which the orbit controls and Equation (4) were applied.

3.4. The ΔV Caculation

The drift rates of each CubeSat were calculated based on the mean orbital elements (MOEs). Classical orbital elements (COEs) are osculating elements that change with orbital perturbations at each instant. Mean orbital elements, which eliminate osculating effects and short periodic variations in Keplerian elements, represent the overall characteristics of the orbit [13]. The variation in the drift rate in an orbital period is derived using MOEs is 10^{-8} rad/s, whereas the variation is 10^{-6} rad/s when COEs are used. The drift rate requires a small change, namely, 10^{-8} rad/s, to operate the orbit for the VISION mission. Therefore, MOEs were used to calculate the drift rate due to the variation of MOEs being smaller than the variation of COEs. The change in MOEs by ΔV cannot be directly derived from the GVEs. Therefore, COEs are used when calculating ΔV based on Equation (4). Alternatively, the drift rates of each CubeSat and the desired change in the drift rate were calculated using Equations (5), (6), and (8) by MOEs.

Figure 8 presents the flowchart for deriving ΔV for three types of orbit controls: drift recovery, station keeping, and reconfiguration. All types of orbit controls start by calculating the drift rates of the two CubeSats in the AoL based on the MOEs with an orbit determination error. For the drift recovery, the difference in the AoL between two CubeSats was calculated, and the desired drift rate of the deputy to reduce the difference in the desired duration was then determined. The desired drift rate of the deputy for the station keeping should be the same as the drift rate of the reference, to maintain the relative distance. For the reconfiguration, the relative AoL corresponding to the relative distance to be changed was calculated. Then, the desired drift rate of deputy CubeSat for changing the relative AoL during transfer time was derived. After determining the desired drift rate, the GVEs and linearized drift rate equation were utilized to compute ΔV based on COEs with orbit determination errors.

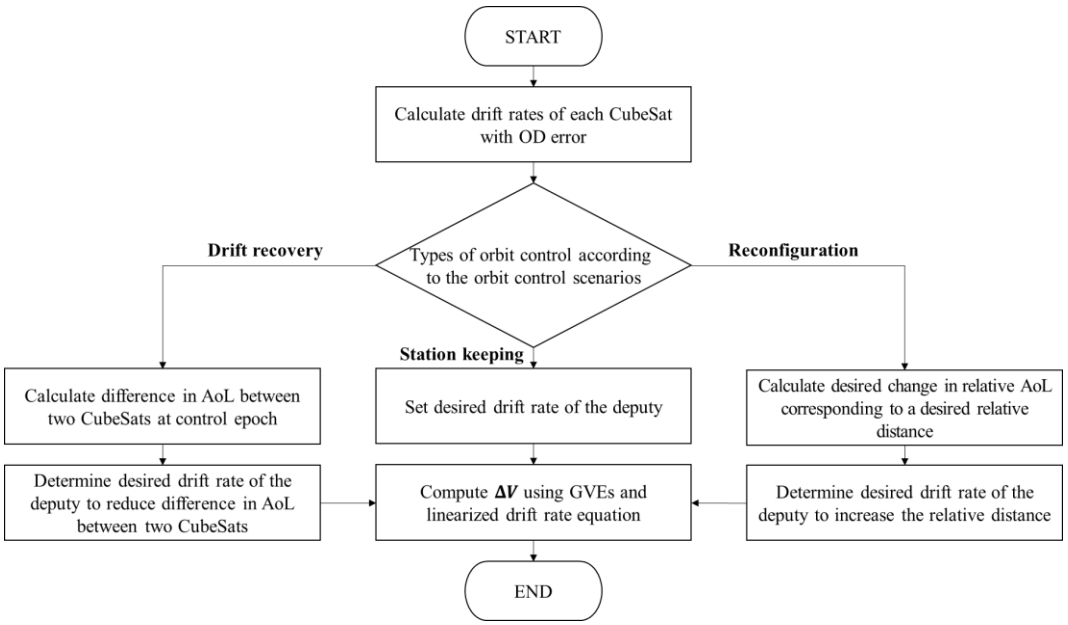

Figure 8. Flowchart of the method to compute ΔV of three types of orbit controls. There are three types of methods to determine the desired drift rate of the deputy CubeSat according to the orbit control types. Moreover, OD denotes orbit determination.

4. Numerical Simulations

4.1. Simulation Setting

To simulate the intended environments, the orbits were propagated by including various orbital perturbations such as air drag, solar radiation pressure, and third body perturbations using the General Mission Analysis Tool (GMAT) developed by NASA [14]. The mass of each CubeSat was approximately 12 kg, and the cross-sectional area of each CubeSat was an average of 0.045 m^2. The COEs of the reference CubeSat at the instant of ejection are listed in Table 1. The orbits of the two CubeSats were near-circular sun-synchronous orbit. The epoch of the COEs was 1 March 2023 12:00:00. The right ascension of the ascending node (RAAN) was determined such that the LTAN was 90° at the epoch. Similar results were expected if RAAN was selected, such that the LTAN was 90° at other epochs. The relative speed of the deputy CubeSat with respect to the reference CubeSat was assumed to be 1 m/s, and the separation angle was assumed to be 80° from the along-track axis on the along- and cross-track planes. Thus, the relative speed in the along-track direction was 0.17 m/s, which influenced the change in the relative distance between the two CubeSats. The altitude of the reference was 600 km, and the orbit was a sun-synchronous orbit. The total ΔV budget was limited to 5 m/s. The standard deviations of the orbit determination errors in the position and velocity were analyzed within the ranges of 1–10 m and 0.001–0.01 m/s along each axis, respectively. According to [15], the velocity uncertainty is approximately 1/1000 of the position uncertainty. Orbital determination errors influenced the ΔV calculation. The transfer speed between the relative distance ranges was set as 20 km/day, and the minimum transfer time was set as 10 days. Therefore, the transfer times between the set points were determined as 10 days, 10 days, 15 days, and 25 days for the mission.

Table 1. Assumed classical orbital elements of reference CubeSat at the ejection from a launch vehicle. The relative velocity of the deputy CubeSat was 0.17 m/s in the along-track direction. The COE is the classical orbital element, the SMA is the semi-major axis, the ECC is eccentricity, the INC is the inclination, the RAAN is the right ascension of ascending node, the AoP is the argument of perigee, and the MA is the mean anomaly.

COE	SMA	ECC	INC	RAAN	AoP	MA
Value	6978 km	0.0001	97.8°	256°	315°	45°

4.2. Ideal Case—Without Orbit Determination and ΔV Errors

To verify whether the proposed orbit control scenarios and methods satisfied the mission objectives, numerical simulations were performed under the assumption that there was no error in the orbital information and ΔV application. Figure 9 presents the changes in relative distance with respect to time. Thirty days after ejection from a launch vehicle, the relative distance between the two CubeSats increased to 1350 km. Subsequently, for the mission, the relative distance was adjusted via multiple orbit controls using the impulsive maneuvers proposed in this study. To demonstrate laser communication at various relative distances, the maneuvers were executed 10 times, and the accumulated ΔV was 0.9281 m/s. All the ΔV**s** acted in a direction parallel to the **S**-axis, as it was the most efficient direction for changing the drift rate by ΔV. The **R**-axis and **W**-axis components of ΔV calculated using the proposed method were zero. The magnitudes in the **S**-axis direction of each ΔV are listed in Table 2. The variations in the relative distances at all set points (50 km, 100 km, 200 km, 500 km, and 1000 km) were less than 2 km over 10 days for each demonstration duration, as shown in Figure 9. Based on numerical simulations, it was verified that the relative distance can be maintained within ±10 km for 10 days at all set points using a ΔV budget of less than 5 m/s for the VISION mission.

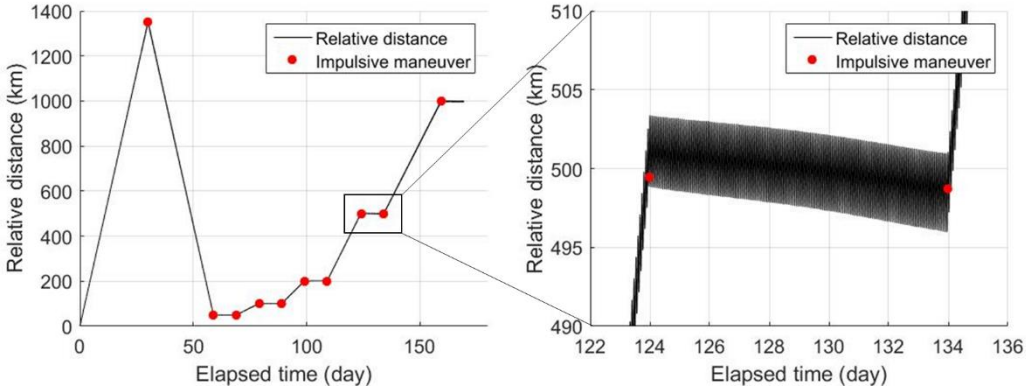

Figure 9. Changes in the relative distance between two CubeSats over time. Ten times of impulsive orbit controls modulated the relative distances and maintained them for 10 days of the demonstration duration at each set point, to demonstrate the laser communication at the various relative distances. The graph on the right-hand side is an enlarged view of the change in the relative distance at 500 km throughout the demonstration duration.

Table 2. The ΔV_S in each orbit control. All ΔVs acted in a direction parallel to the **S**-axis. After the drift recovery to decrease the relative distance, the station keeping and reconfiguration were repeated to change and maintain the set point.

Orbit Control	Objective	ΔV_S (m/s)
#1	Drift recovery	−0.3499
#2	Station keeping	0.1761
#3	Reconfiguration	0.0194
#4	Station keeping	−0.0196
#5	Reconfiguration	0.0386
#6	Station keeping	−0.0388
#7	Reconfiguration	0.0774
#8	Station keeping	−0.0784
#9	Reconfiguration	0.0774
#10	Station keeping	−0.0772
Accumulated ΔV (magnitude)		0.9281 m/s

Figure 10 presents the angle between the relative position vectors of the two CubeSats and sun vectors over time. The angles oscillated at approximately 90°. This was because the RAAN was set such that the LTAN was 90°, to minimize the noise generated by the sunlight incident on the optical system. In particular, if the RAAN was 256° in the initial epoch, an orbit perpendicular to the sun vector shown in Figure 3 was formed. Considering the effect on the mission, the angle between the sunlight and relative position vector should range from 70–110°. Thus, the proposed orbit satisfied this requirement.

The **S**-axis separation velocity of the two CubeSats after ejection from a launch vehicle influenced the ΔV magnitude, given that the relative distance increased further within the same duration according to the **S**-axis separation velocity. It was validated that the ΔV budget could be satisfied even when the orbit was controlled in the worst case, assuming that the separation speed of 1 m/s acted in the **S**-axis direction. Figure 11 presents the variation in the relative distance between the two CubeSats. The relative distance increased to 7400 km after the ejection. The accumulated magnitude of ΔV was 3.4535 m/s for 10 impulsive controls, which was less than the desired ΔV budget. The magnitudes of ΔV of the drift recovery and the first station keeping were 1.6639 m/s and 0.8373 m/s, respectively. The magnitude of ΔV for the drift recovery and first station keeping increased when compared with the results shown in Figure 9 and Table 2 for the ideal case. This is because the desired change in the drift rate increased via the drift recovery and first station keeping orbit controls.

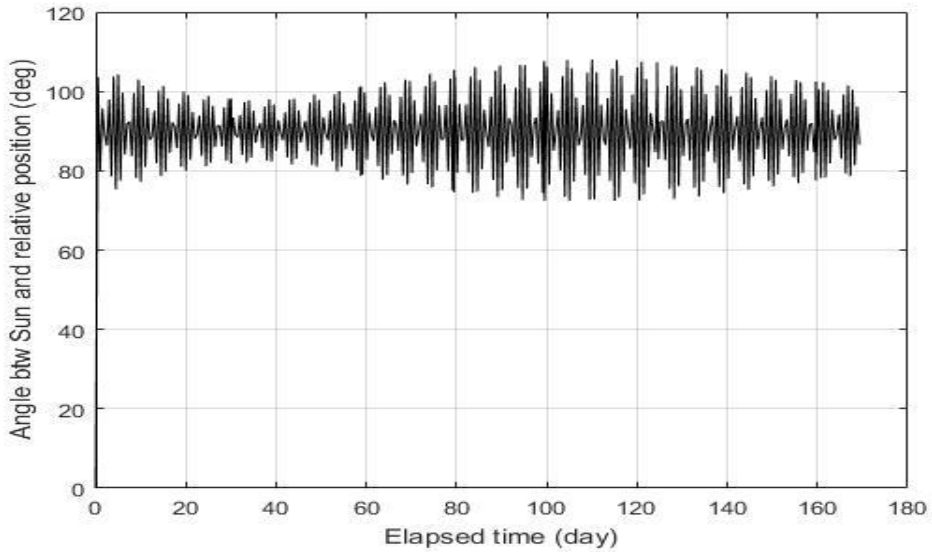

Figure 10. The angle between the sun vector and relative position vector of the two CubeSats according to the elapsed time. The angles were near 90° for the elapsed time. This indicates that the orbit was maintained to minimize the sunlight incident on the optical system during the mission.

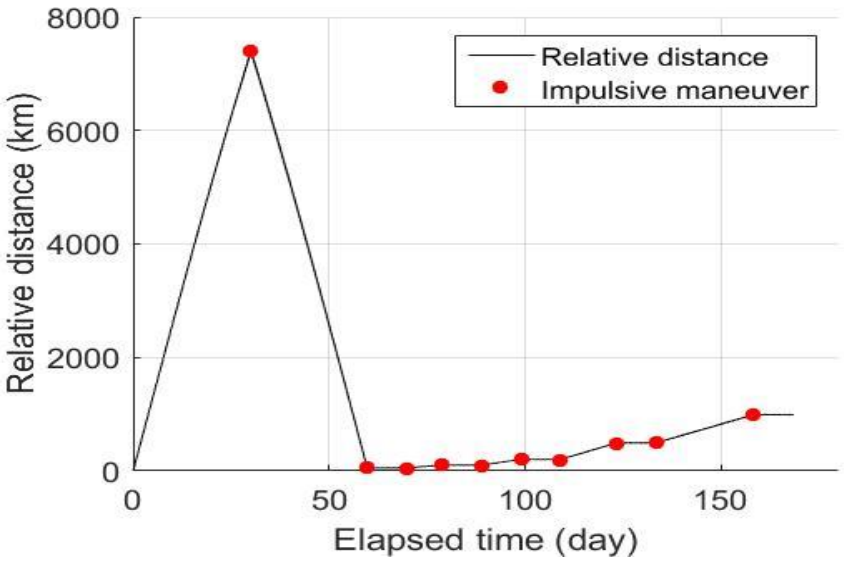

Figure 11. Changes in the relative distance between two CubeSats over time when the relative speed after the ejection was 1 m/s (assumed worst case) in the along-track direction. The maximum relative distance reached 7400 km. The accumulated magnitude of ΔV was 3.45 m/s, which satisfied the given ΔV budget.

4.3. Discussion on the Orbit Determination Errors

For the VISION mission, precise orbit determination (POD) was performed to estimate the position and velocity of a CubeSat with high accuracy based on global navigation satellite system (GNSS) observations. In the case of low earth orbit small satellites (GRACE and Sentinel-3), the position accuracy was at the sub-decimeter level and the average velocity root mean square error was within 0.05 mm/s [16]. In addition, CubeSat, which cannot track GNSS signals continuously due to power constraints, demonstrated a similar level of POD results only in post-processing [17]. For the VISION mission, the standard deviation of the position error was assumed to be 1.5 m along each axis, which was demonstrated by OEM719, a GPS receiver produced by NovAtel. The standard deviation of the velocity error was assumed to be 0.003 m/s with respect to the analysis in [16] and

margin. In this section, it was assumed that ΔV was generated with orbit determination errors, and ΔV was provided by thrusters without errors in its magnitude and direction.

The set points could not be precisely maintained during the mission, as shown in Figure 12, due to the errors in the position and velocity caused by the orbit determination errors. This error causes orbital information errors such as orbital element errors. The errors influenced the calculation of the drift rates of the two CubeSats and that of ΔV of the deputy CubeSat. The errors in the orbital information caused errors in the MOE used to calculate the drift rates of the two CubeSats. In addition, the errors in the orbital information led to errors in the coefficient of Equation (4) that was used to calculate ΔV. For the case reflecting the orbit determination errors, the maximum change in the relative distance for 10 days was 8.7 km at 500 km of the set point in the simulation. This change satisfied the requirement of the orbit controls to maintain the relative distance over the demonstration duration within $\pm$ 10 km. In this case, the accumulated magnitude of ΔV was 0.9293 m/s, which was less than the ΔV budget. The ΔV_S for each orbit control is shown in Table 3. The orbit determination errors yielded an error of $\sim 10^{-3}$ m/s in the magnitude of ΔV. Hence, the orbit determination errors led to minimal fluctuations in the precise maintenance of the set points. However, it is necessary to determine the acceptable range of orbit determination errors to satisfy mission requirements.

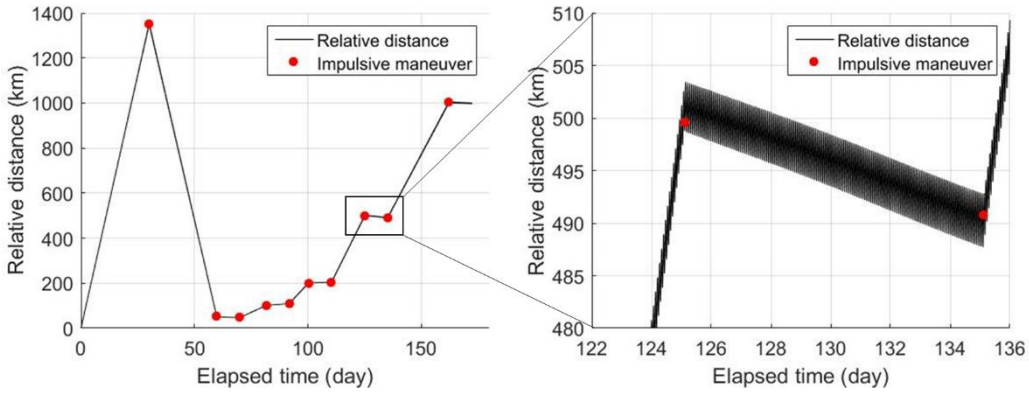

Figure 12. Changes in the relative distances between the two CubeSats over time for the case including the orbit determination errors.

Table 3. The ΔV_S in each orbit control for the case including the orbit determination error.

Orbit Control	Objective	ΔV_S (m/s)	Differences from Table 2 (m/s)
#1	Drift recovery	−0.3542	-4.3568×10^{-3}
#2	Station keeping	0.1669	-9.1752×10^{-3}
#3	Reconfiguration	0.0193	-8.8801×10^{-7}
#4	Station keeping	−0.0072	1.2367×10^{-2}
#5	Reconfiguration	0.0387	2.7177×10^{-5}
#6	Station keeping	−0.0318	7.0297×10^{-3}
#7	Reconfiguration	0.0775	3.1428×10^{-5}
#8	Station keeping	−0.0773	1.1510×10^{-3}
#9	Reconfiguration	0.0774	-6.9649×10^{-5}
#10	Station keeping	−0.0791	-1.8690×10^{-3}
Accumulated ΔV (magnitude)		0.9293	5.1347×10^{-3}

4.4. Analysis of Influences Caused by Orbit Determination Errors

Large orbit determination errors can influence the mission performance to maintain relative distances within $\pm$ 10 km. The influences of increasing the orbit determination errors on ΔV and relative distance change after the station keeping were analyzed to determine the requirements for the errors. For the simulations, the position error was increased in

intervals of 1 m from 1–10 m, and the velocity error was set as 0.001–0.01 m/s. In the case of orbit control for the first station keeping, the simulation was performed including errors. For each error, 100 Monte Carlo simulations were performed. Figure 13a presents the change in the magnitude of the required ΔV as the orbit determination errors increased. Figure 13b presents the change in the relative distance over 10 days according to the errors in the orbital information. As can be seen from Figure 13, the dots indicate the averages of 100 simulations, and the error bars indicate the standard deviation. If there was no error, the relative distance after the station keeping changed slightly. As the orbit determination errors increased, the change in the set point increased with an increase in the error in ΔV. To maintain the set point within $\pm$10 km, the change in the relative distance should be less than 20 km. Therefore, as shown in Figure 13b, the orbit determination errors of the position and velocity should be less than 4 m and 0.004 m/s for each axis, to maintain the set point within $\pm$10 km. The proposed requirements for orbit determination errors can be satisfied by using a precise orbit determination method based on the Global Positioning System (GPS) data received by the receiver mounted on the VISION mission.

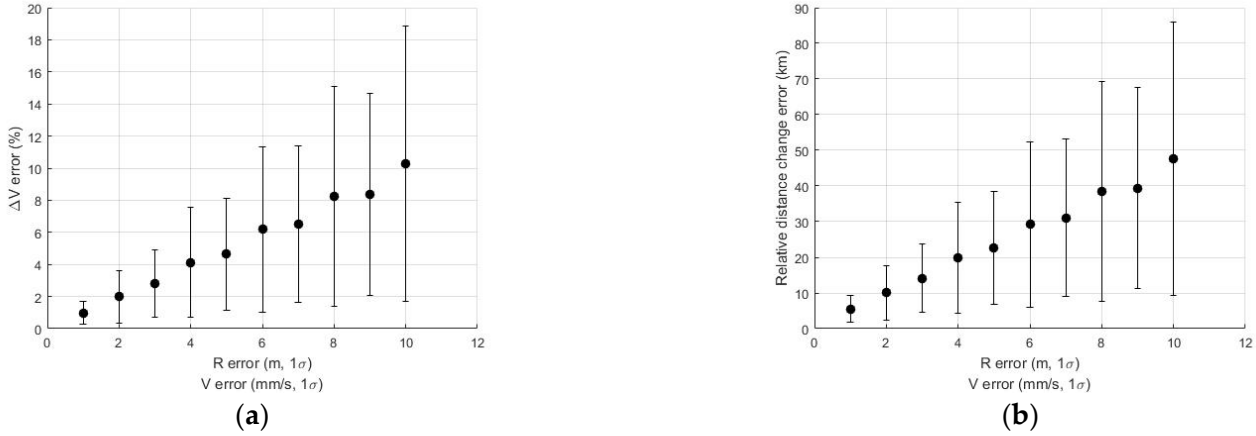

Figure 13. The ΔV errors and changes in the relative distances according to the orbit determination errors. The two parameters increased as the position and velocity errors increased. (**a**) The ΔV differences compared with the ideal case. (**b**) Changes in the relative distance according to the orbit determination errors.

4.5. Analysis of Influences due to ΔV Error

The magnitude and direction errors in ΔV can be caused by manufacturing and structural errors and can influence orbital operations. The thrust magnitude error was caused by the manufacturing error of the thrust nozzle. The thrust direction error was caused by the structural error and attitude control errors of the CubeSat, given that the thrust module was fixed on the CubeSat body. The thrust direction error means the angle between the desired thrust direction and the applied thrust direction. Figure 14a,b indicates the changes in relative distance after the station was maintained according to the increase in the thrust magnitude and direction error, respectively. As shown in Figure 14a, the thrust magnitude error influenced the change in the relative distance after the station keeping. As shown in Figure 14b, the thrust direction error influenced the change in the relative distance after the station keeping by reducing ΔV, which acts in the along-track direction. However, it was insignificant when compared with the influence of the thrust magnitude error. Therefore, the magnitude and direction error of ΔV should be less than 4% (1σ) and 5° (1σ), respectively, to meet the mission requirements.

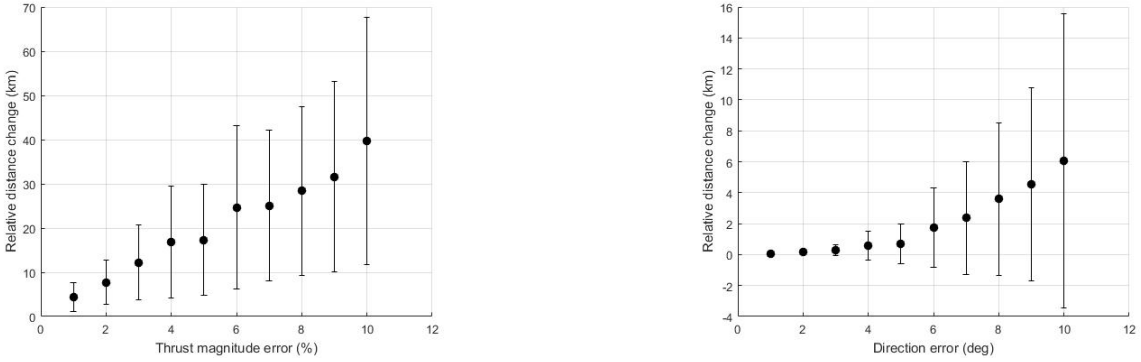

Figure 14. The changes in the relative distances according to the thrust magnitude error (**a**) and direction error (**b**). The thrust magnitude error increased the changes in the relative distances. The thrust direction error changed the relative distances by reducing ΔV_S.

4.6. Analysis of Influences due to Time Synchronization Error

The time synchronization error denotes the time difference between the epoch of the orbital information used to determine the orbit control and the time required to generate the thrust. The time difference is caused by the computational speed and delays of the data communication between the electrical devices mounted in CubeSat. The proposed algorithm to calculate ΔV in this study did not require significant computation time. In addition, if ΔV is calculated on the ground and transmitted as a command to CubeSat, a time synchronization error occurs due to the clock error of the CubeSat. Figure 15 presents the changes in the relative distance between the two CubeSats after 10 days according to the time synchronization errors. The origin in Figure 15 represents the result when there was no time error. Even when there was no time synchronization error, the relative distance changed by 0.0636 km for 10 days, as it could not be maintained due to various perturbations. When the orbit was controlled before the epoch of the orbital information used to calculate ΔV, the changes in the relative distances decreased. When controlled later, the changes in the relative distances increased. This is because the changes in the drift rate by a fixed ΔV differed depending on the AoL at which orbit control was conducted. Nevertheless, the difference in the relative distances due to the time synchronization error was approximately 0.03 km for 10 days. Given that the mission requirement was to maintain the relative distance within $\pm$10 km for 10 days, the time synchronization error had a slight influence on the mission performance.

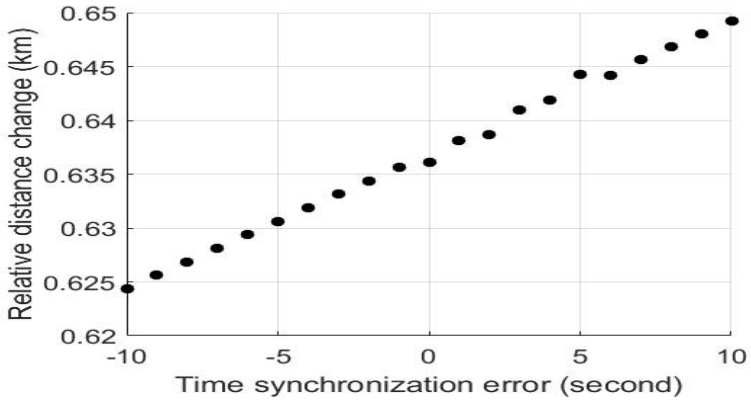

Figure 15. The changes in the relative distances according to the time synchronization error. The changes in the relative distance due to the error were insignificant.

4.7. Performance with Respect to All the Errors

To reflect actual environments, various errors were considered for the orbit control simulations. The standard deviations (1σ) of the position and velocity were set as 1.5 m (1σ) and 0.003 m/s (1σ) along each axis, respectively, and the errors in the thrust magnitude and direction were 1 % (1σ) and 3° (1σ), respectively. The time synchronization error was not considered, as it had slight influence on the relative distance changes. Figure 16 presents the changes in relative distances according to the orbit controls. The relative MOE is shown in Figure 17. The relative distance between satellites is changed or maintained due to differences in drift rates caused from differences in SMA. The accumulated magnitude of $\boldsymbol{\Delta V}$ was 0.9318 m/s, and the maximum change in the relative distance for 10 days was 13.4 km at the set point of 500 km in this case of the simulation. Even with realistic errors, it was confirmed that orbital operations can meet the mission requirements.

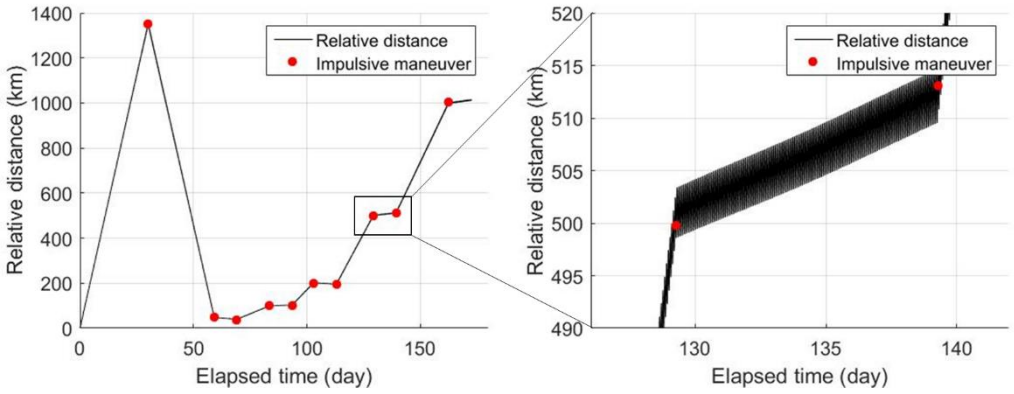

Figure 16. Changes in the relative distance between two CubeSats over time with respect to the errors in the orbit determination and thrust magnitude and direction. The standard deviation (1σ) of the position and velocity along each axis was 1.5 m and 0.003 m/s, respectively. The thrust magnitude and direction errors were 1% (1σ) and 3° (1σ), respectively. The set points were maintained within $\pm$10 km.

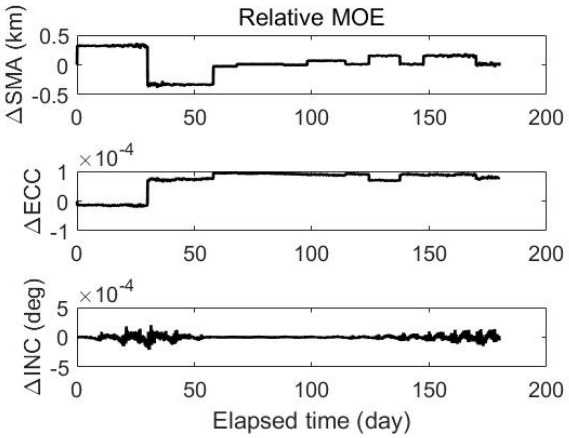

Figure 17. Relative mean orbital elements with respect to the elapsed time. The difference in SMA causes the difference in the drift rate to modulate the relative distance.

4.8. Relative Distance Control between Different Satellites

To date, the control methods proposed in this study have been applied to two identical CubeSats. The appropriate conditions for the application of the methods to CubeSats with different properties were investigated, as presented in this section. It was assumed that two CubeSats with different masses and sizes attempted to control their relative distances for the establishment of inter-satellite links. The mass and cross-sectional area of the reference CubeSat were set as 12 kg and 0.045 m^2, respectively, and the mass of the deputy was set as

6 kg. The mass-to-area ratio of the deputy ranged from 0.7–1.3. A ratio of 1.0 implies that the area of the deputy CubeSat with half the mass of the reference CubeSat is 0.0225 m^2. Orbit control was performed to maintain the relative distances at 100 km using the drift rate modulation. The initial state vectors of the two CubeSats were set up for both CubeSats immediately after the third orbit control, as described in Section 4.2. The relative distances between the CubeSats with different masses and sizes were influenced by the different air drag forces. Figure 18 presents the relative distances between the two CubeSats over time according to the mass-to-area ratio. The times required to reach a relative distance of 100 km were different, given that the relative distances varied due to the different air drag forces according to the mass-to-area ratio, as shown in Table 4. When the ratio exceeded 1.3, the relative distance did not reach 100 km, which was the target distance. In addition, even after the orbit was controlled to maintain the relative distances, the relative distances were not maintained; however, they were increased or decreased by the differential air drag between the two CubeSats. If the mass-to-area ratio is the same for the two CubeSats, although they have different masses and sizes, the drift rate modulation proposed in this study can be used to precisely control the relative distances.

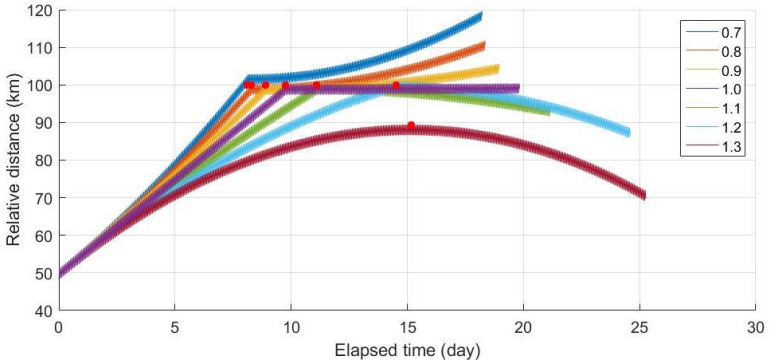

Figure 18. The changes in the relative distance between CubeSats with different mass-to-area ratios over time. The time required to reach a relative distance of 100 km and the changes in the relative distance after the station keeping (red dots on figure) varied according to the mass-to-area ratio.

Table 4. The simulation results for the relative distance controls between CubeSats with different mass-to-area ratios. The influence of the mass-to-area ratio with respect to the reference CubeSat on the time required to reach the target relative distance and the changes in the relative distance after the station keeping.

Mass-to-Area Ratio w.r.t Reference CubeSat	Time Required to Reach 100 km (days)	Changes in Relative Distance after 10 Days (km)
0.7	8.12	18.5498
0.8	8.28	10.5978
0.9	8.89	4.3278
1.0	9.75	0.0369
1.1	11.09	−7.3268
1.2	14.53	−13.4146
1.3	Not reached	−19.7132

5. Conclusions

This paper proposes the VISION mission, which comprises an orbital control strategy implemented in various scenarios to verify laser communication in space. The mission consists of two CubeSats that change and maintain their relative distance. In this study, we designed the method for controlling the relative distances for the practical mission by adjusting the drift rate using impulsive control. Based on the analysis results for the magnitude of the orbital zonal harmonics' terms that influence the drift rate, the drift rate was calculated by considering only the linear term of J_2. Based on numerical simu-

lations, the feasibility of orbital operation was confirmed within a ΔV budget of 5 m/s using the proposed orbit control method in various orbital control scenarios. The relative position vectors were maintained nearly perpendicularly to the sun vector for all time periods, to minimize the noise caused by sunlight. In addition, the influences of the orbit determination error, ΔV error, and time synchronization error were analyzed. The changes in the relative distance after the station keeping increased with an increase in the orbit determination error. To satisfy the mission requirement of maintaining the relative distance for 10 days within $\pm$10 km, the errors of the position and velocity should be less than 4 m and 4 mm on each axis, respectively. The thrust magnitude and direction errors influenced the changes in the relative distance after the station keeping, which maintained the set points. The thrust magnitude error was found to have a more significant influence than the thrust direction error, which should be less than 5% to maintain the relative distance within $\pm$10 km. The time synchronization error had a negligible effect on maintaining the relative distance. The mass-to-area ratio between CubeSats with different properties should be the same to control the relative distance using drift rate modulation. In this study, the influences of various errors on the maintenance of the relative distance were analyzed. Since impulsive burn is assumed, it is less realistic than the case of orbit control by simulating finite burn considering the performance of the thruster. Hence, the levels of error were dependent on the precision of the relative distance maintenance required for the mission. In addition, this approach can be utilized for more precise orbit control simulations considering several constraints derived from the CubeSat development for the VISION mission. Furthermore, the results presented in this paper can be utilized for the realization of a megaconstellation of multiple satellites with different properties.

Author Contributions: Conceptualization, Y.S., G.-N.K. and S.-Y.P.; methodology, Y.S. and D.-G.K.; software, Y.S.; validation, Y.S. and S.-Y.P.; formal analysis, Y.S.; investigation, Y.S., G.-N.K. and D.-G.K.; resources, Y.S., G.-N.K. and S.-Y.P.; writing—original draft preparation, Y.S. and G.-N.K.; writing—review and editing, Y.S. and S.-Y.P.; supervision, S.-Y.P.; project administration, S.-Y.P.; funding acquisition, S.-Y.P. All authors have read and agreed to the published version of the manuscript.

Funding: This research was supported by the Defense Challengeable Future Technology Program of Agency for Defense Development, Republic of Korea (grant number: UD200029RD).

Institutional Review Board Statement: Not applicable.

Informed Consent Statement: Not applicable.

Conflicts of Interest: The authors declare no conflict of interest.

References

1. Kaushal, H.; Jain, V.K.; Kar, S. *Free Space Optical Communication: Review Paper*; Springer: Berlin/Heidelberg, Germany, 2017.
2. Toyoshima, M. Recent Trends in Space Laser Communications for Small Satellites and Constellations. *J. Light. Technol.* **2021**, *39*, 693–699. [CrossRef]
3. Long, M.J. Pointing Acquisition and Tracking Design and Analysis for CubeSat Laser Communication Crosslinks. Master's Thesis, Massachusetts Institute of Technology, Cambridge, MA, USA, 2018.
4. Cahoy, K.; Grenfell, P.; Crews, A.; Long, M.; Serra, P.; Nguyen, A.; Fitzgerald, R.; Haughwout, C.; Diez, R.; Aguilar, A.; et al. The CubeSat Laser Infrared CrosslinK Mission (CLICK). *Proc. SPIE* **2018**, *11180*, 33. [CrossRef]
5. Welle, R.P.; Coffman, C.; Pack, D.W.; Santiago, J.R. CubeSat Laser Communication Crosslink Pointing Demonstration. In Proceedings of the 33rd Annual AIAA/USU Conference on Small Satellites, Utah State University, Logan, UT, USA, 16 July 2019; p. 9.
6. Leboffe, E.M.; Howard, T.; Freeman, A.P.; Robie, D. Multi-mission capable 1550 nm lasercom terminal for space applications. *Proc. SPIE* **2020**, *11272*, 4. [CrossRef]
7. Dolkens, D. A deployable telescope for sub-meter resolutions from microsatellite platforms. Master's Thesis, Delft TU, Delft, The Netherlands, 2015.
8. Lee, Y.; Park, S.Y.; Park, J.P.; Song, Y. Numerical analysis of relative orbit control strategy for CANYVAL-X mission. *J. Astron. Space Sci.* **2019**, *36*, 235–248. [CrossRef]
9. Walker, R. GOMX-4—The twin European mission for IOD purposes. In Proceedings of the 32nd Annual AIAA/USU Conference Small Satellite, Logan, UT, USA, 6–9 August 2018; p. SSC18-VII–07.

10. Song, Y.; Park, S.-Y.; Lee, S.; Kim, P.; Lee, E.; Lee, J. Spacecraft formation flying system design and controls for four nanosats mission. *Acta Astronaut.* **2021**, *186*, 148–163. [CrossRef]
11. Vallado, D.A.; McClain, W.D. *Fundamentals of Astrodynamics and Applications*, 2nd ed.; McGraw-Hill Companies, Inc.: New York, NY, USA, 1997. [CrossRef]
12. Battin, R.H. *An Introduction to the Mathematics and Methods of Astrodynamics*; AIAA Education Series: New York, NY, USA, 1999.
13. Walter, H.G. Conversion of osculating orbital elements into mean elements. *Astron. J.* **1967**, *72*, 994. [CrossRef]
14. Hughes, S.P.; Qureshi, R.H.; Cooley, D.S.; Parker, J.J.K.; Grubb, T.G. Verification and validation of the general mission analysis tool (GMAT). In Proceedings of the AIAA/AAS Astrodynamics Specialist Conference, San Diego, CA, USA, 4−7 August 2014. [CrossRef]
15. Teunissen, P.J.G.; Montenbruck, O. (Eds.) *Springer Handbook of Global Navigation Satellite Systems*; Springer International Publishing: Berlin/Heidelberg, Germany; Cham, Switzerland, 2017.
16. Allahvirdi-Zadeh, A.; Wang, K.; El-Mowafy, A. POD of small LEO satellites based on precise real-time MADOCA and SBAS-aided PPP corrections. *GPS Solut.* **2021**, *25*, 1–14. [CrossRef]
17. Wang, K.; Allahvirdi-Zadeh, A.; El-Mowafy, A.; Gross, J.N. A sensitivity study of POD using dual-frequency GPS for CubeSats data limitation and resources. *Remote Sens.* **2020**, *12*, 2107. [CrossRef]